Am J Transl Res 2025;17(12):9555-9565
www.ajtr.org /ISSN:1943-8141/AJTR0169226

Original Article

Tirzepatide alleviates non-alcoholic fatty liver disease by regulating lipid metabolism through activation of the AMPK/NF-κB signaling pathway

Pengfei Wu[1*], Hao Xu[2*], Yuqiao Zeng[2], Ao Shen[1], Cheng Zhang[1], Bing Wu[1], Xinyue Zhang[1], Han Zhang[1], Yiyu He[3], Likun Wang[2]

[1]School of Clinical Medicine, Shandong Second Medical University, Weifang 261053, Shandong, China; [2]Infection Control Center, Linyi People's Hospital, Linyi 276000, Shandong, China; [3]Department of Cardiovescular Disease, Renmin Hospital of Wuhan University, Wuhan 430060, Hubei, China. [*]Equal contributors and co-first authors.

Received October 10, 2025; Accepted December 4, 2025; Epub December 15, 2025; Published December 30, 2025

Abstract: Background: Non-alcoholic fatty liver disease (NAFLD) is a prevalent metabolic disorder with limited therapeutic options. Tirzepatide (TZP), a novel dual agonist, has shown promise in metabolic disease, but its effects and mechanisms in NAFLD remain unclear. Methods: Human HepG2 cells were treated with palmitate (PA) to induce steatosis and then exposed to various concentrations of TZP. Mouse were treated with high-fat diet (HFD) to establish a NAFLD model in vivo, followed by TZP treatment. NAFLD-related indicators including cell viability, intracellular lipid accumulation, serum biochemical parameters, glucose homeostasis, inflammation, oxidative stress, and hepatic histopathology were evaluated. The AMP-activated protein kinase (AMPK)/nuclear factor κB (NF-κB) pathway and lipid metabolism-related protein were analyzed. Results: TZP suppressed PA-induced lipid accumulation, triglyceride and total cholesterol content, cell apoptosis, while it enhanced cell viability in HepG2 cells. In HFD-induced NAFLD mice, TZP treatment markedly decreased liver weight, attenuated hepatic steatosis, ballooning, and necrosis, and abnormal lipid accumulation by inhibiting insulin resistance, inflammatory cytokines, oxidative stress, and hepatic fibrosis markers. Mechanistically, TZP modulated the AMPK/NF-κB pathway by increasing p-AMPK and decreasing p-NF-κB levels, leading to downregulation of lipogenic genes. Conclusion: TZP effectively improved hepatic steatosis, inflammation, oxidative stress, and fibrosis in experimental NAFLD models through the AMPK/NF-κB pathway.

Keywords: Tirzepatide, non-alcoholic fatty liver disease, AMPK/NF-κB pathway, lipid metabolism

Introduction

Non-alcoholic fatty liver disease (NAFLD) is a highly prevalent metabolic disorder primarily involving excessive fat accumulation in the liver, inflammatory flare-ups, and ultimately leading to liver fibrosis [1, 2]. The whole pathogenesis of NAFLD is driven by multiple factors, including a complex interplay between metabolic dysregulation, insulin resistance, genetic predisposition, and environmental factors [3, 4]. It is not surprising that NAFLD usually appears at the same time as obesity and type 2 diabetes, because they all have the common characteristics of metabolic syndrome, such as chronic inflammation and universal insulin resistance [1]. Despite the increasing burden and prevalence of NAFLD, there are currently no approved drug therapies specifically targeting NAFLD. It is crucial to have a deeper understanding of the actual mechanisms driving the progression of NAFLD and to identify effective therapeutic drugs and targeted therapy strategies.

Tirzepatide (TZP), abbreviated as TZP, is a dual agonist that acts on both glucagon like peptide-1 (GLP-1) and glucose dependent insulinotropic polypeptide (GIP) receptors. It has shown great promise in the treatment of various metabolic diseases and receptor agonists, as well as in metabolic diseases [5, 6]. TZP seems to improve the core metabolic problems of type 2 diabetes and obesity through a series of different actions, such as stimulating insulin secretion in a way that depends on glucose lev-

https://doi.org/10.62347/SNZK2023

els, inhibiting abnormally high levels of glucagon, slowing the speed of gastric emptying, and working in the brain to suppress appetite [7, 8]. TZP has been approved by the US Food and Drug Administration for the treatment of type 2 diabetes. However, in addition to diabetes, in the field of cardiovascular disease, TZP also seems to help alleviate cardiac dysfunction, mainly by inhibiting oxidative stress and inflammation [9, 10]. In animal models, such as HFD induced obese mice, treatment with TZP significantly improved insulin resistance and fatty liver condition, i.e. hepatic steatosis [11]. In this regard, new evidence suggests that TZP can also inhibit the expression of certain biomarkers associated with non-alcoholic fatty liver disease and even liver fibrosis [12]. Given all these related findings, the impact of TZP on NAFLD remains an unresolved issue that has not been very well explored.

AMP activated protein kinase (AMPK) is a threonine protein kinase that is fundamentally the main sensor of energy balance in mammalian cells. Its impact is very extensive, and it participates in the regulation of the entire cellular function in almost every type of tissue. It has always been related to how the body manages glucose, lipids, and protein metabolism, not to mention its role in gene expression and overall growth. The accumulated evidence suggests that AMPK activation reduces SREBP-1c and FAS activity, thereby inhibiting metabolic processes such as cholesterol and TAG biosynthesis. Interestingly, AMPK acts as an upstream regulator of NF-κB, inhibiting its activation and thereby participating in NAFLD progression.

In this study, we aimed to assess the therapeutic potential of TZP in NAFLD models and to dig into the underlying mechanisms behind it. Using PA-induced HepG2 cells and a HFD-induced mouse model, the effects of TZP on hepatic lipid accumulation, inflammation, oxidative stress and AMPK/NF-κB pathway was evaluated. Finally, this study provides insights into the molecular mechanisms of TZP in NAFLD and highlights its potential as a novel therapeutic drug.

Materials and methods

Cell culture, free fatty acid induction, and tirzepatide treatment

The HepG2 cells were obtained from ATCC (USA) and were cultured in DMEM supplemented with 10% FBS and 1% penicillin-streptomycin (Beyotime, China) at 37°C in a 5% CO_2 atmosphere.

To establish the cellular steatosis model, HepG2 cells were first exposed to palmitate (PA; Sigma-Aldrich, USA) at a concentration of 1 mM for a full 24 h to reliably induce lipid accumulation. Following this lipid-loading phase, the same cells were then exposed to TZP (MedChemExpress, USA) at 50 nM or 100 nM concentrations for an additional 24 h to assess its effects. Control groups received vehicle treatment (PBS with 1% BSA).

Cell viability assay

After treatment, HepG2 cells were incubated with CCK-8 reagent (10% v/v) for 2 h at 37°C. Absorbance was measured at 450 nm using a microplate reader.

Oil red O staining

HepG2 Cells were fixed with 4% paraformaldehyde for 20 min, incubated with Oil Red O working solution (Sigma-Aldrich) for 30 min, and then counterstained with hematoxylin. Images were captured using an inverted microscope (Nikon, Japan), and lipid droplets were quantified by extracting stained Oil Red O with isopropanol and measuring absorbance at 510 nm.

Intracellular Triglyceride (TG) and Total Cholesterol (TC) measurements

Cellular TG and TC levels were determined using commercial assay kits (Applygen, China and Biosino, China, respectively). After treatment, cells were lysed, and the supernatant was collected. Absorbance was read at 550 nm (TG) and 500 nm (TC) following the manufacturer's protocols.

Quantitative Real-Time PCR (qRT-PCR)

Total RNA was extracted from HepG2 cells using TRIzol reagent (Invitrogen, USA). cDNA was synthesized using a PrimeScript RT reagent kit (Takara, Japan). qRT-PCR was performed with SYBR Green Premix (Roche, Switzerland) on a QuantStudio 5 system (Applied Biosystems, USA). Relative expression for SREBP-1c, PPARα, FAS, SCD1, and GAPDH (internal control) was calculated using the $2^{-\Delta\Delta Ct}$ method. The PCR primer sequences are shown in **Table 1**.

Table 1. Sequences of primers used in PCR

Gene	Primer sequences (5'-3')
SREBP-1c	F: CTTAGAGCGAGCACTGAACTGTGTG
	R: CTGGAACTGATGGAGAAGCTGTAGG
PPARα	F: TATTCGGCTGAAGCTGGTGTAC
	R: CTGGCATTTGTTCCGGTTCT
FAS	F: GCGGGTTCGTGAAACTGATAA
	R: GCAAAATGGGCCTCCTTGATA
SCD1	F: TCTTCCTTATCATTGCCAACACCA
	R: GCGTTGAGCACCAGAGTGTATCG
GAPDH	F: GGGAAGCTTGTCATCAATGG
	R: TGGACTCCACGACGTACTCA

Animal model and drug administration

To establish a murine model of NAFLD, 6-week-old male C57BL/6J mice (Vital River Laboratory) were subjected to a 12-week dietary regimen after acclimation. The animals were randomly segregated into two groups: a control diet (CD, 10% kcal fat) group and a HFD (60% kcal fat) group. Subsequently, HFD-fed mice were treated with tirzepatide (10 nmol/kg/day, subcutaneous injection) or vehicle (saline) for 4 weeks. Mouse body weights were measured weekly. Following anesthesia by isoflurane (2%, 0.5 L/min), the weight was immediately recorded. Upon completion of retro-orbital bleeding and subsequent euthanasia by cervical dislocation, the livers were promptly excised. After a saline rinse and careful drying with filter paper, the liver weight was recorded. Animal experimental procedures were granted approval by the Institutional Animal Care and Use Committee of the Linyi people's hospital.

Histological analysis of liver tissues

Liver tissues were fixed in 4% paraformaldehyde, embedded in paraffin, and sectioned at 5 μm thickness. Hematoxylin and eosin (H&E) staining was performed for morphological evaluation. Frozen sections were used for Oil Red O staining to visualize lipid accumulation. Images were acquired with a light microscope (Nikon, Tokyo, Japan). The severity of NAFLD was assessed using the well-established NAFLD Activity Score (NAS) system by two experienced pathologists who were blinded to the group assignments [13].

Serum biochemical analysis

Biochemical profiling of serum samples, including TC, TG, LDL-C, HDL-C, ALT, and AST, was performed. The analyses were conducted on a Mindray (China) automated biochemical analyzer with corresponding commercial kits, using blood collected from the orbital vein after fasting.

Hepatic inflammatory and oxidative stress markers

Liver tissues were homogenized in cold PBS. Contents of TNF-α, IL-6, SOD, MDA, and glutathione (GSH) were quantified utilizing ELISA kits (R&D Systems, USA) and biochemical assay kits according to manufacturers' instructions.

Oral Glucose Tolerance Test (OGTT), Fasting Blood Glucose (FBG), and insulin measurement

After 6 hours of fasting, mice were administered glucose (2 g/kg, orally). Blood glucose levels were measured at 0, 30, 60, 90, and 120 min using a glucometer (Roche, Basel, Switzerland). FBG and serum insulin levels were determined with ELISA kits (Millipore, USA). Homeostatic model assessment of insulin resistance (HOMA-IR) was calculated as: [fasting glucose (mmol/L) × fasting insulin (mU/L)]/22.5.

Western blot analysis

Liver tissues were lysed in RIPA buffer containing protease inhibitors. Proteins were separated by SDS-PAGE and transferred to PVDF membranes. After blocking, membranes were incubated with primary antibodies against SREBP-1c (1:1500), PPARα (1:2000), FAS (1:1200), SCD1 (1:1500), AMPK (1:1000), NF-κB (1:1000), and GAPDH (1:5000), followed by HRP-conjugated secondary antibodies. ECL reagent (Millipore) and ImageJ software was utilized to visualize and analyze for bands.

Statistical analysis

Statistical analysis was performed using Prism 8 software (LLC, San Diego, CA, USA). Count data were presented as mean ± standard deviation (SD) and analyzed using t-tests between two groups, preceded by a test for equality of variances. If variances were equal, independent-samples t-tests were applied; if unequal, nonparametric independent-samples tests were used. For comparisons among multiple gr-

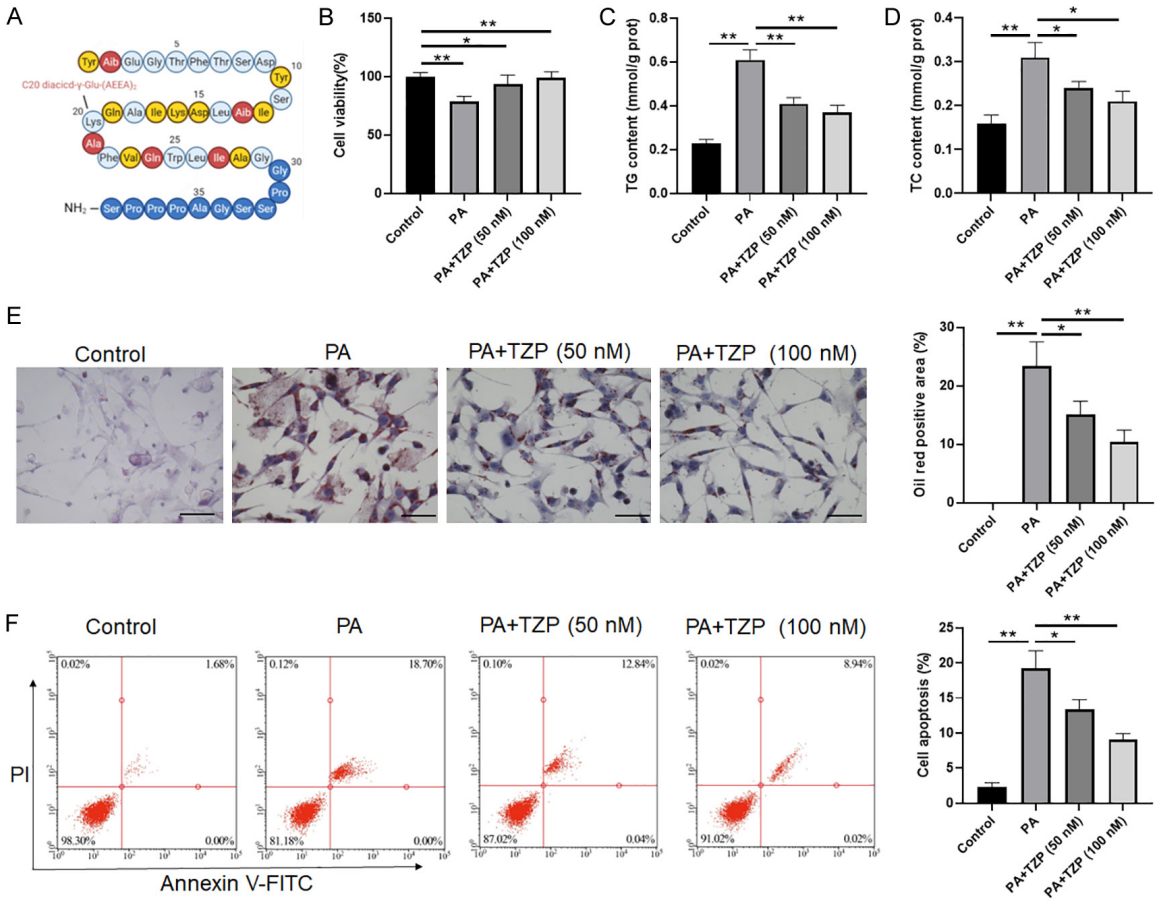

Figure 1. TZP treatment reduces lipid accumulation in HepG2 cell stimulated by PA. A. The structure of TZP. B. Cell viability of HepG2 cells was assessed by CCK-8 assay after TZP treatment. C and D. Cell TG and TC content of HepG2 cells were assessed by relative kits after TZP treatment. E. Cell Oil Red O staining of HepG2 cells after TZP treatment. Scale bar = 50 μm. F. Cell apoptosis of HepG2 cells were assessed by flow cytometry after TZP treatment. *P < 0.05, **P < 0.01.

oups, one-way analysis of variance (ANOVA) was performed followed by Tukey's post hoc test. For data involving two independent factors (e.g., diet and drug treatment), two-way ANOVA was applied followed by Sidak's post hoc test. For the OGTT data, which were measured at multiple time points in the same animals, repeated measures two-way ANOVA was used. Differences were considered statistically significant at $P < 0.05$.

Results

TZP treatment reduces lipid accumulation in HepG2 cells stimulated by PA

TZP consists of 39 amino acids and contains a C18 fatty acid side chain, as shown in **Figure 1A**. To evaluate the therapeutic potential of TZP in NAFLD, we conducted in vitro experiments using PA-stimulated HepG2 cells. TZP treatment effectively ameliorated the PA-induced reduction in cell viability (**Figure 1B**). Furthermore, both TG and TC contents were decreased in PA-treated HepG2 cells following administration of different concentrations of TZP, with higher doses producing more pronounced effects (**Figure 1C** and **1D**). Oil Red O staining revealed a significant increase in the percentage of stained area in PA-stimulated cells, which was markedly attenuated by TZP treatment (**Figure 1E**). In addition, TZP treatment effectively reversed PA-induced apoptosis (**Figure 1F**). These findings indicate that TZP has the potential to reduce lipid accumulation in HepG2 cells induced by PA stimulation.

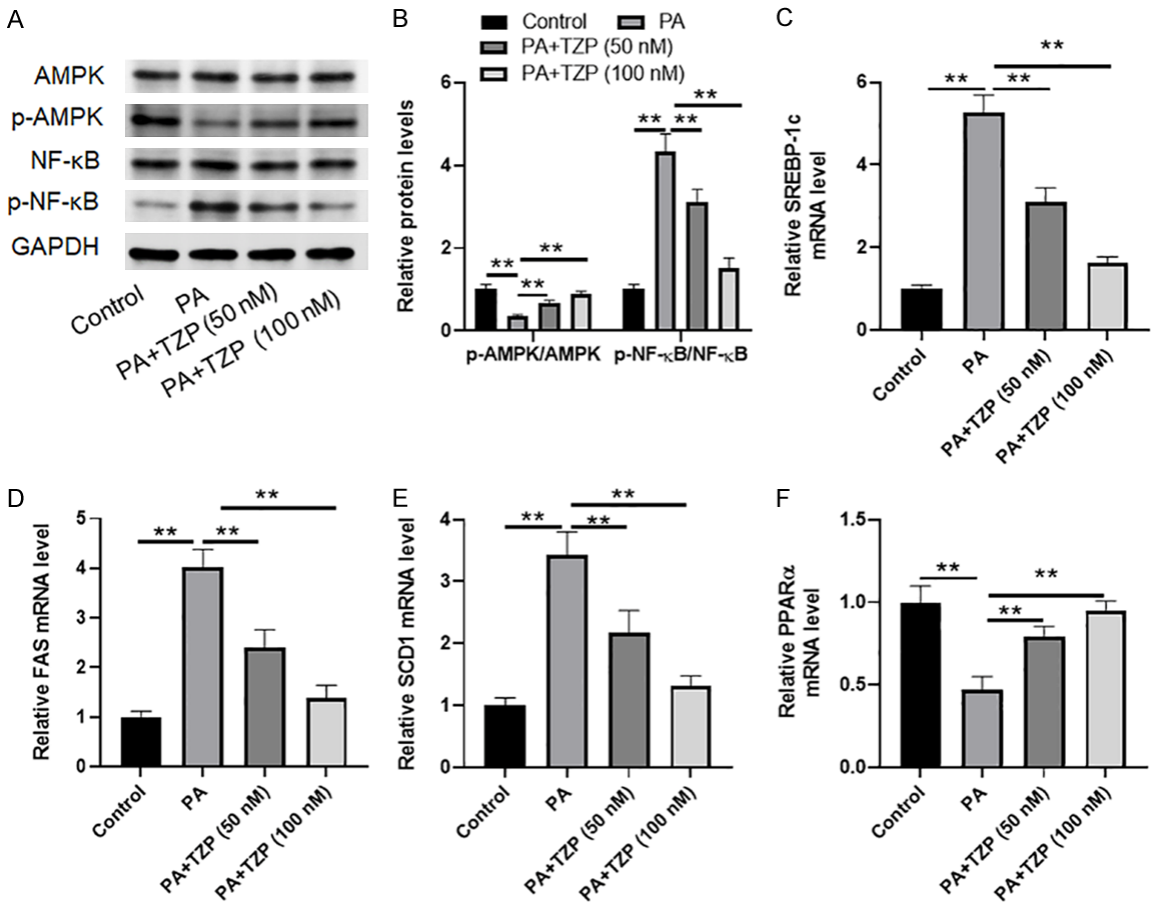

Figure 2. The effect of TZP on lipid metabolism in NAFLD is mediated by the AMPK/NF-κB pathway. A and B. Cell p-AMPK and p-NF-κB levels of PA-induced HepG2 cells were assessed by western blot assay after TZP treatment. C-F. Cell SREBP1-1c, SCD1, FAS and PPARα levels of PA-induced HepG2 cells were assessed by qRT-PCR assay after TZP treatment. **P < 0.01.

The effect of TZP on lipid metabolism in NAFLD is mediated by the AMPK/NF-κB pathway

Since the AMPK/NF-κB pathway may play a crucial role in abnormal lipid metabolism in the liver, the effect of TZP for the AMPK/NF-κB pathway was investigated in vitro. TZP treatment effectively reduced AMPK phosphorylation levels in PA-stimulated HepG2 cells, resulting in a significant increase in NF-κB phosphorylation (**Figure 2A** and **2B**). Next, we investigated whether TZP regulates lipid metabolism by modulating the AMPK/NF-κB pathway. In PA-treated HepG2 cells, the lipid synthesis-related markers SREBP1-1c, SCD1 and FAS expression was remarkably elevated, while TZP diminished both SREBP1-1c, SCD1 and FAS expression (**Figure 2C-E**). In addition, TZP increased levels of the PPARα in HepG2 treated with PA (**Figure 2F**).

TZP mitigates liver injury in NAFLD mice fed HFDs

To examine the efficacy of TZP on NAFLD in vivo, mice were fed a HFD for 12 weeks. Based on HE and Oil red O staining results, we uncovered that the HFD mice exhibited improved lipid accumulation and hepatocyte swelling and necrosis after TZP treatment, which was confirmed by Oil red positive area and NAFLD Activity Score (**Figure 3A** and **3B**). After 4 weeks of TZP treatment, the liver weight and liver-to-body weight ratio were diminished in HDF mice (**Figure 3C** and **3D**). Moreover, serum levels of AST and ALT in the HFD group were increased, while these levels were significantly reduced in the TZP treatment group (**Figure 3E** and **3F**).

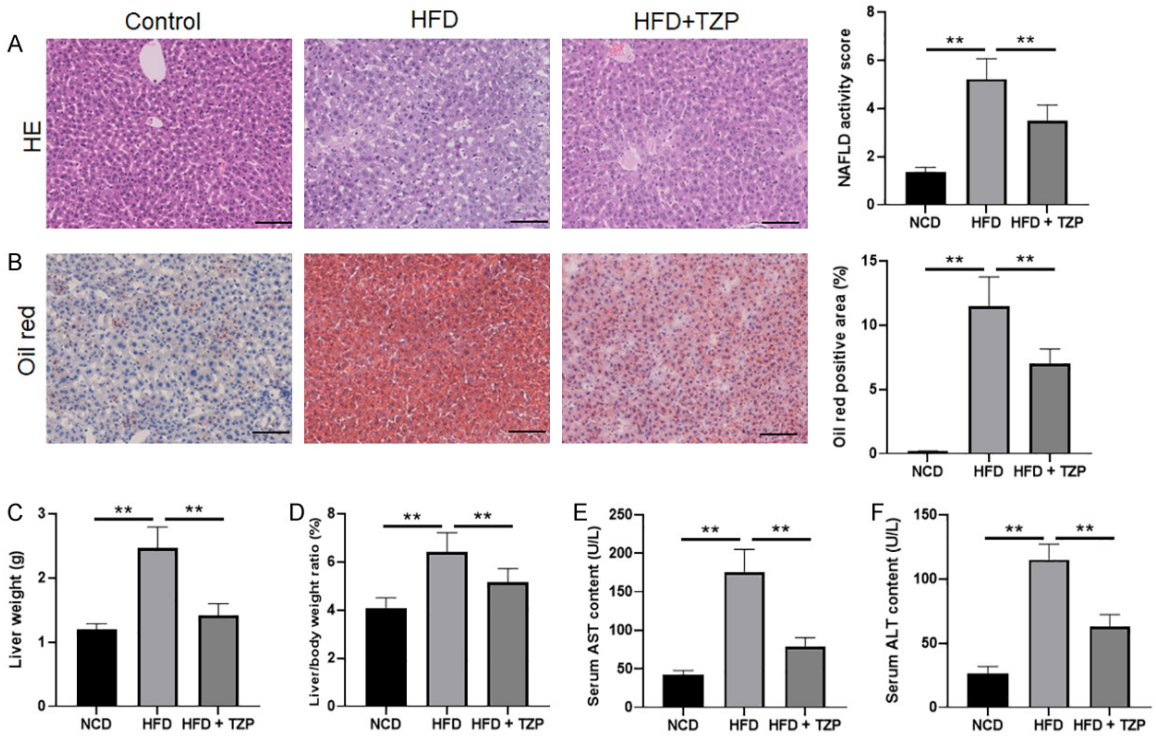

Figure 3. TZP mitigates liver injury in mice with HFD-induced NAFLD mice. A and B. Detection of liver weight and liver/body weight ratio (%). Scale bar = 50 μm. C. HE staining of mouse liver tissue and calculation of NAFLD activity Score (n = 7). D. Oil red O staining of mouse liver tissue and calculation of oil red positive area (n = 7). E and F. Serum contents of AST and ALT in mice (n = 7). **P < 0.05.

TZP alleviates dyslipidemia and insulin resistance in NAFLD mice fed HFDs

We further examined the concentrations of TG, TC, LDL-C, HDL-C, and FFA to analyze the effects of TZP on serum lipid profiles in mice across experimental groups. Relative to the NCD group, mice fed a HFD exhibited markedly abnormal lipid parameters, consistent with the induction of hyperlipidemia. On the contrary, TZP treatment effectively diminished TG, TC, LDL-C, and FFA content, while increasing HDL-C content compared with the mice fed a HFD (**Figure 4A-E**). Next, the serum glucose, FBG, fasting insulin levels, and HOMA-IR index were evaluated to assess insulin resistance. The TZP-treated group demonstrated significantly lower FBG and HOMA-IR values relative to the HFD group, with levels approaching those observed in the NCD group (**Figure 4F-I**). The data displayed that TZP administration exerts hypoglycemic effects and improves glucose tolerance in mice.

TZP mitigates liver inflammation, fibrosis and oxidative stress in NAFLD mice fed HFDs

Although the inflammatory factor content of TNF-α and IL-6 was increased in livers, induced by HFD, TZP treatment could reverse the HFD-mediated promoting effects (**Figure 5A** and **5B**). With the continued consumption of a HFD, mice with NAFLD not only exhibit liver inflammatory damage but also developed fibrosis. Compared to those of NCD mice, higher fibrosis-related markers Col1a1, Col3a1, and Acta2 levels were observed in HFD fed mice, which were visibly reversed in the liver after TZP treatment (**Figure 5C**). Moreover, oxidative stress examination indicated that TZP treatment facilitated SOD and GSH secretion, and suppressed MDA in HFD mice (**Figure 5D-F**).

TZP reduces NAFLD in mice fed HFDs by inhibiting the AMPK/NF-κB pathway

We further examined whether TZP critically contributed to HFD-induced abnormal lipid metab-

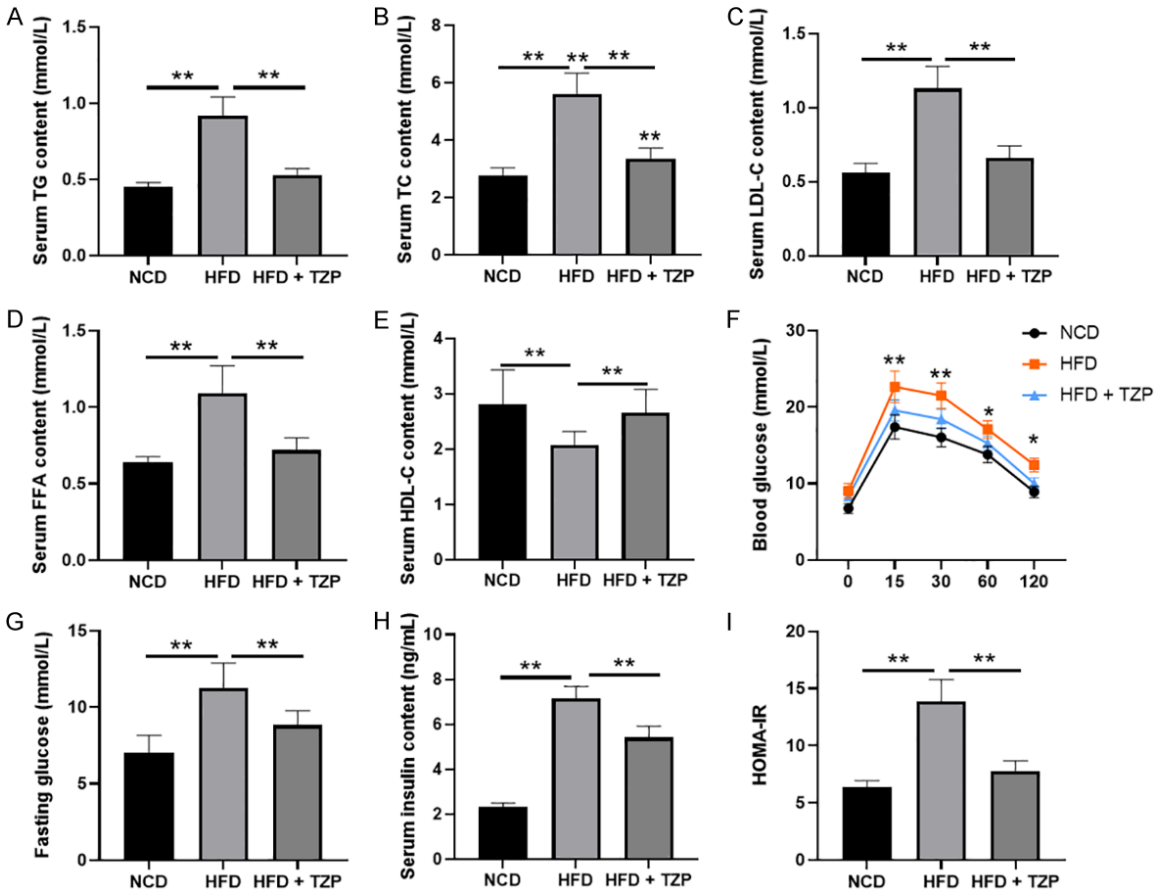

Figure 4. TZP alleviates dyslipidemia and insulin resistance in NAFLD mice with HFD. A-E. Detection of serum TG, TC, LDL-C, FFA and HDL-C levels in mice after TZP treatment (n = 7). F-I. Detection of serum glucose, FBG, fasting insulin levels, and HOMA-IR index in mice after TZP treatment (n = 7). *P < 0.05, **P < 0.01.

olism via the AMPK/NF-κB pathway in mice. The results depicted that the inhibitory effects of a HFD on p-AMPK and the promoting impact of a HFD on p-NF-κB vanished in TZP-treated mice with NAFLD (**Figure 6A-C**). Moreover, a similar inhibitory effects of TZP on SREBP1-1c and FAS protein levels were observed in NAFLD mice (**Figure 6D-F**), suggesting TZP is involved in the inhibition of lipid synthesis by signaling in the AMPK/NF-κB pathway.

Discussion

The present study demonstrates that TZP treatment effectively ameliorates hepatic steatosis and improves metabolic parameters in both PA-induced HepG2 cells and HFD-induced NAFLD mice. These beneficial effects are likely mediated through the modulation of the AMPK/NF-κB signaling pathway, resulting in enhanced lipid metabolism, reduced inflammation and oxidative stress, and improved insulin sensitivity.

The compound TZP has garnered considerable research interest due to its recurrent association with various metabolic disorders. Empirical data consistently demonstrate its efficacy in suppressing key lipid markers, namely cholesterol and triglycerides, thereby offering a potential therapeutic strategy to ameliorate these dysregulated metabolic patterns [14]. After long-term injection of TZP into the brain ventricles of mice, the ratio of white and brown adipose tissue changed, accompanied by a significant increase in lipid metabolism rate [15]. An increasing number of studies are linking TZP to liver-related diseases, encompassing conditions ranging from MASH and liver fibrosis to hepatocellular carcinoma [16]. Mice with metabolic dysfunction-associated fatty liver disease improved liver injury by reducing fatty acid

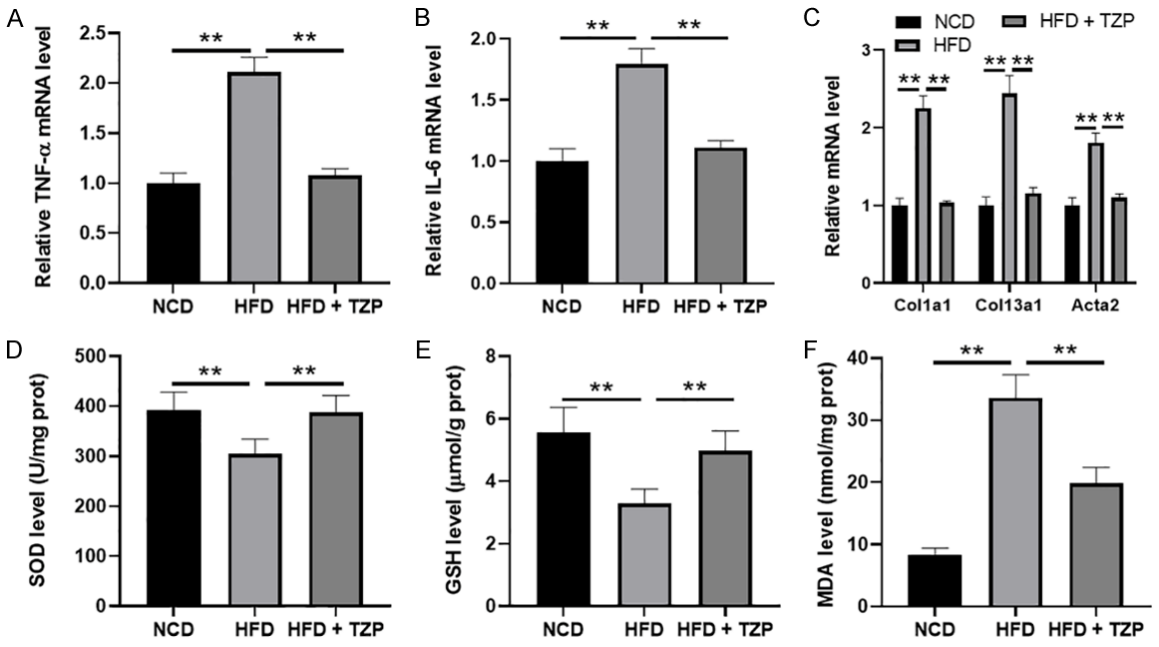

Figure 5. TZP mitigates liver inflammation, fibrosis and oxidative stress in NAFLD mice with HFD. A and B. Detection of TNF-α and IL-6 contents in mice after TZP treatment (n = 7). C. Detection of Col1a1, Col3a1, and Acta2 mRNA levels in mice after TZP treatment. D-F. Detection of SOD, GSH and MDA contents in mice after TZP treatment (n = 7). **P < 0.01.

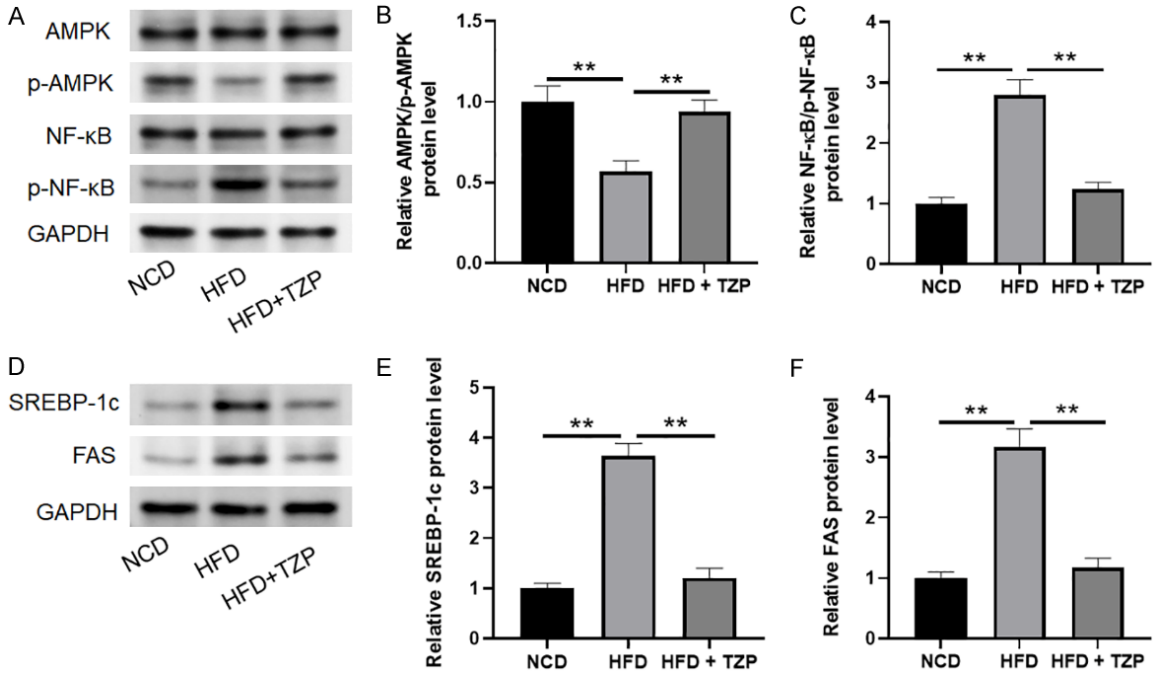

Figure 6. TZP reduces NAFLD in mice with HFD by inhibiting the AMPK/NF-κB pathway. A-C. Liver p-AMPK and p-NF-κB levels of mice were assessed by western blotting after TZP treatment (n = 7). D-F. Liver SREBP1-1c and FAS levels of mice were assessed by western blotting after TZP treatment (n = 7). **P < 0.01.

uptake and promoting cholesterol efflux through TZP administration [17]. Given all these cumulative findings from the aforementioned literature, the present work used TZP to investi-

gate its functional role within the context of HFD-induced NAFLD. In HepG2 cells, TZP exposure markedly improved overall cell viability and clearly reduced intracellular lipid buildup. Meanwhile, administering TZP markedly attenuated hepatic steatosis, ballooning, and necrosis in the HFD-induced NAFLD mouse model, as confirmed by detailed tissue analysis, corresponding drops in key liver injury markers (ALT, AST), improvements in dyslipidemia parameters (TG, TC, LDL-C), and better readings on blood glucose metrics (FBG, insulin). Our findings that TZP alleviates hepatic steatosis, dyslipidemia, and insulin resistance in HFD-fed mice are consistent with the known metabolic benefits of this dual agonist. For instance, Hartman et al. demonstrated in a clinical setting that TZP administration led to significant reductions in biomarkers associated with nonalcoholic steatohepatitis (NASH) and liver fibrosis in patients with type 2 diabetes [12].

AMPK is a central regulator of cellular energy homeostasis and is a major player in how lipids are metabolized, where its activation sets off a couple of key downstream pathways. It catalyzes and promotes the actual breakdown of lipids, such as fatty acid beta oxidation, while on the other hand, it actively inhibits lipid synthesis, just like the entire de novo lipid synthesis process [18]. When AMPK is activated in the liver, the result is fatty acid oxidation, while glucose, fat, and protein synthesis are generally inhibited [19]. Previous studies have shown that activating AMPK can effectively limit triglyceride accumulation and oxidative stress burden in rats fed HFD [20, 21]. Enhancing AMPK phosphorylation accelerates triglyceride metabolism and reduces oxidative stress, thereby helping to improve fatty degeneration of liver [22]. Here, we observed that TZP-mediated reduction in p-AMPK was accompanied by downregulation of SREBP1-1c, SCD1, FAS, MDA, and concurrent upregulation of PPARα, SOD and GSH, which enhances fatty acid β-oxidation. Indeed, NF-κB has been implicated in hepatic steatosis in NAFLD through modulation of inflammation [23]. Inflammatory cytokines promote peripheral lipolysis, hepatic steatosis, inflammation, necrosis, and apoptosis, leading to the development of NAFLD [24]. Accumulating research has revealed that the regulation of the AMPK/NF-κB signaling pathway is a key mechanism in NAFLD [22, 25-27]. For example, Cai et al. reported that p-synephrine ameliorated NAFLD by regulating the liver-adipose axis via the AMPK/NF-κB pathway, similarly resulting in the downregulation of SREBP-1c and FAS [22]. Moreover, Ma et al. found that TZP mitigates the harmful effects of a HFD by suppressing oxidative stress and inflammation [28]. Here, TZP increased p-AMPK and decreased p-NF-κB, leading to of lipogenic proteins SREBP-1c and FAS downregulation. This pathway is central to the regulation of lipid metabolism, inflammation, and oxidative stress in NAFLD. The activation of AMPK promotes fatty acid oxidation and suppresses lipogenesis, while the inhibition of NF-κB reduces inflammatory cytokine production and oxidative stress markers. The consistent inhibitory impact of TZP on the AMPK/NF-κB pathway across both cellular and animal models underscores its mechanism of action. Our research findings extend these findings by identifying the clinically approved drug TZP as a potent activator of this beneficial pathway. In addition, although GLP-1 receptor agonists such as liraglutide have also been shown to activate AMPK in the liver [29], the dual GIP/GLP-1 receptor activation of TZPs may lead to more effective or synergistic activation, which can explain their significant efficacy in our model and clinical trials of weight loss and blood glucose control [8].

Notwithstanding the promising findings of this study, a significant limitation must be acknowledged. Although the AMPK/NF-κB pathway was identified as a key mechanistic mediator, the precise molecular mechanisms through which TZP activates AMPK have not been determined and thus remain a critical area for future investigation. Future studies should employ targeted experimental approaches, such as AMPK knockout models and specific pharmacological modulators (agonists and antagonists), to establish a definitive causal link between AMPK activation and the pharmacological effects of TZP.

In conclusion, TZP exhibits multi-faceted protective effects against NAFLD by modulating lipid metabolism, reducing inflammation and oxidative stress, and improving insulin sensitivity, largely through the AMPK/NF-κB pathway. These findings highlight the therapeutic potential of TZP acting as a candidate for NAFLD treatment. Future studies should focus on elu-

cidating its precise molecular targets and evaluating its long-term efficacy and safety in preclinical and clinical settings.

Acknowledgements

This study was supported by the Natural Science Foundation of Shandong Province (No. ZR2021MH375), and the TCM Science and Technology Key Project of Shandong Province (No. Z-2022036).

Disclosure of conflict of interest

None.

Address correspondence to: Yiyu He, Department of Cardiovescular Disease, Renmin Hospital of Wuhan University, No. 238 Jiefang Road, Wuchang District, Wuhan 430060, Hubei, China. E-mail: Heyiyu09160@126.com; Likun Wang, Infection Control Center, Linyi People's Hospital, No. 27 Jiefang Road, Lanshan District, Linyi 276000, Shandong, China. E-mail: Lkwang999@163.com

References

[1] Marjot T, Moolla A, Cobbold JF, Hodson L and Tomlinson JW. Nonalcoholic fatty liver disease in adults: current concepts in etiology, outcomes, and management. Endocr Rev 2020; 41: bnz009.

[2] Powell EE, Wong VW and Rinella M. Non-alcoholic fatty liver disease. Lancet 2021; 397: 2212-2224.

[3] Geng Y, Faber KN, de Meijer VE, Blokzijl H and Moshage H. How does hepatic lipid accumulation lead to lipotoxicity in non-alcoholic fatty liver disease? Hepatol Int 2021; 15: 21-35.

[4] Buzzetti E, Pinzani M and Tsochatzis EA. The multiple-hit pathogenesis of non-alcoholic fatty liver disease (NAFLD). Metabolism 2016; 65: 1038-48.

[5] Syed YY. Tirzepatide: first approval. Drugs 2022; 82: 1213-1220.

[6] France NL and Syed YY. Tirzepatide: a review in type 2 diabetes. Drugs 2024; 84: 227-238.

[7] Jastreboff AM, Aronne LJ, Ahmad NN, Wharton S, Connery L, Alves B, Kiyosue A, Zhang S, Liu B, Bunck MC and Stefanski A; SURMOUNT-1 Investigators. Tirzepatide once weekly for the treatment of obesity. N Engl J Med 2022; 387: 205-216.

[8] Frías JP, Davies MJ, Rosenstock J, Pérez Manghi FC, Fernández Landó L, Bergman BK, Liu B, Cui X and Brown K; SURPASS-2 Investigators. Tirzepatide versus semaglutide once weekly in patients with type 2 diabetes. N Engl J Med 2021; 385: 503-515.

[9] Liu Q, Zhu J, Kong B, Shuai W and Huang H. Tirzepatide attenuates lipopolysaccharide-induced left ventricular remodeling and dysfunction by inhibiting the TLR4/NF-kB/NLRP3 pathway. Int Immunopharmacol 2023; 120: 110311.

[10] Yang D, Chen YH, Chen YK, Zeng YL and Ling ZY. Tirzepatide alleviates doxorubicin-induced cardiotoxicity via inhibiting HRD1-mediated Nrf2 ubiquitination. Cardiovasc Res 2025; 121: 1865-1882.

[11] Wang R, Lin Z, He M, Liao Y, Xu Y, Chen C, Duan X, Jiang X and Qiu J. The role of gut microbiota in Tirzepatide-mediated alleviation of high-fat diet-induced obesity. Eur J Pharmacol 2025; 1002: 177827.

[12] Hartman ML, Sanyal AJ, Loomba R, Wilson JM, Nikooienejad A, Bray R, Karanikas CA, Duffin KL, Robins DA and Haupt A. Effects of novel dual GIP and GLP-1 receptor agonist tirzepatide on biomarkers of nonalcoholic steatohepatitis in patients with type 2 diabetes. Diabetes Care 2020; 43: 1352-1355.

[13] Kleiner DE, Brunt EM, Van Natta M, Behling C, Contos MJ, Cummings OW, Ferrell LD, Liu YC, Torbenson MS, Unalp-Arida A, Yeh M, McCullough AJ and Sanyal AJ. Design and validation of a histological scoring system for nonalcoholic fatty liver disease. Hepatology 2005; 41: 1313-21.

[14] Mahar MU, Mahmud O, Ahmed S, Qureshi SA, Kakar WG and Fatima SS. The effects of tirzepatide on lipid profile: a systematic review and meta-analysis of randomized controlled trials. J Obes Metab Syndr 2024; 33: 348-359.

[15] Zhang A, Liu Q, Xiong Y, Li J, Xu Y, Song H, Jing X, Xu H, Yang N, Li Y, Mo L, Tang Q and He J. Tirzepatide reduces body weight by increasing fat utilization via the central nervous system-adipose tissue axis in male mice. Diabetes Obes Metab 2025; 27: 2844-2856.

[16] Jeong BK, Choi WI, Choi W, Moon J, Lee WH, Choi C, Choi IY, Lee SH, Kim JK, Ju YS, Kim P, Moon YA, Park JY and Kim H. A male mouse model for metabolic dysfunction-associated steatotic liver disease and hepatocellular carcinoma. Nat Commun 2024; 15: 6506.

[17] Liang J, Liu H, Lv G, Chen X, Yang Z, Hu K and Sun H. Exploring the molecular mechanisms of tirzepatide in alleviating metabolic dysfunction-associated fatty liver in mice through integration of metabolomics, lipidomics, and proteomics. Lipids Health Dis 2025; 24: 8.

[18] von Loeffelholz C, Coldewey SM and Birkenfeld AL. A narrative review on the role of AMPK on de novo lipogenesis in non-alcoholic fatty liver

disease: evidence from human studies. Cells 2021; 10: 1822.
[19] Yang YM, Han CY, Kim YJ and Kim SG. AMPK-associated signaling to bridge the gap between fuel metabolism and hepatocyte viability. World J Gastroenterol 2010; 16: 3731-42.
[20] Li Q, Tan JX, He Y, Bai F, Li SW, Hou YW, Ji LS, Gao YT, Zhang X, Zhou ZH, Yu Z, Fang M, Gao YQ and Li M. Atractylenolide III ameliorates non-alcoholic fatty liver disease by activating hepatic adiponectin receptor 1-mediated AMPK pathway. Int J Biol Sci 2022; 18: 1594-1611.
[21] Yang Z, Zhang L, Liu J, Chan ASC and Li D. Saponins of tomato extract improve non-alcoholic fatty liver disease by regulating oxidative stress and lipid homeostasis. Antioxidants (Basel) 2023; 12: 1848.
[22] Cai WF, Chen QC, Ni Q, Liu L, Liu Q, Yi YK, Jiang CP and Shen CY. p-Synephrine ameliorates non-alcoholic fatty liver disease by regulating liver-adipose axis via AMPK/NF-kappa B pathway. J Ethnopharmacol 2025; 348: 119890.
[23] Rohm TV, Meier DT, Olefsky JM and Donath MY. Inflammation in obesity, diabetes, and related disorders. Immunity 2022; 55: 31-55.
[24] Heida A, Gruben N, Catrysse L, Koehorst M, Koster M, Kloosterhuis NJ, Gerding A, Havinga R, Bloks VW, Bongiovanni L, Wolters JC, van Dijk T, van Loo G, de Bruin A, Kuipers F, Koonen DPY and van de Sluis B. The hepatocyte IKK:NF-κB axis promotes liver steatosis by stimulating de novo lipogenesis and cholesterol synthesis. Mol Metab 2021; 54: 101349.
[25] Tian J, Cai M, Jin S, Chen Q, Xu J, Guo Q, Yan Z, Han X and Lu H. JianPi-QingHua formula attenuates nonalcoholic fatty liver disease by regulating the AMPK/SIRT1/NF-κB pathway in high-fat-diet-fed C57BL/6 mice. Pharm Biol 2023; 61: 647-656.
[26] Zhang LJ, Li SY, Fan SL, Nuerbiye A, Zhao JY, Keremu B, Yang L, Zhang K, Wang HY and Wang JH. Hepatoprotective activity of mulberry extract in NAFLD mice for regulating lipid metabolism and inflammation identified via AMPK/PPAR-γ/NF-κB axis. J Ethnopharmacol 2025; 351: 120108.
[27] Geethangili M, Lin CW, Mersmann HJ and Ding ST. Methyl brevifolincarboxylate attenuates free fatty acid-induced lipid metabolism and inflammation in hepatocytes through AMPK/NF-κB signaling pathway. Int J Mol Sci 2021; 22: 10062.
[28] Ma J, Liu Y, Hu J, Liu X, Xia Y, Xia W, Shen Z, Kong X, Wu X, Mao L and Li Q. Tirzepatide administration improves cognitive impairment in HFD mice by regulating the SIRT3-NLRP3 axis. Endocrine 2025; 87: 486-497.
[29] Guo T, Yan W, Cui X, Liu N, Wei X, Sun Y, Fan K, Liu J, Zhu Y, Wang Z, Zhang Y and Chen L. Liraglutide attenuates type 2 diabetes mellitus-associated non-alcoholic fatty liver disease by activating AMPK/ACC signaling and inhibiting ferroptosis. Mol Med 2023; 29: 132.